

Disintegration and reformation of intermediate-shock segments in three-dimensional MHD bow shock flows

H. De Sterck¹

von Karman Institute for Fluid Dynamics, Sint-Genesius-Rode, Belgium
Centre for Plasma Astrophysics, Katholieke Universiteit Leuven, Belgium

S. Poedts

Centre for Plasma Astrophysics, Katholieke Universiteit Leuven, Belgium

Abstract. Recently, it has been shown that for strong upstream magnetic field, stationary three-dimensional magnetohydrodynamic (MHD) bow shock flows exhibit a complex double-front shock topology with particular segments of the shock fronts being of the intermediate MHD shock type. The large-scale stability of this new bow shock topology is investigated. Two types of numerical experiments are described in which the upstream flow is perturbed in a time-dependent manner. It is found that large-amplitude noncyclic localized perturbations may cause the disintegration of the intermediate shocks, which are indeed known to be unstable against perturbations with integrated amplitudes above critical values, but that in the driven bow shock problem there are always shock front segments where intermediate shocks are reformed dynamically, resulting in the reappearance of the new double-front topology with intermediate-shock segments after the perturbation has passed. These MHD results indicate a theoretical mechanism for the possible intermittent formation of shock segments of intermediate type in unsteady space physics bow shock flows when upstream magnetic fields are strong, for example, in the terrestrial bow shock during periods of strong interplanetary magnetic field, which are more common under solar maximum conditions, or in leading shock fronts induced by fast coronal mass ejections in the solar corona. It remains to be confirmed if intermediate-shock segments would be formed when kinetic effects and realistic dissipation in real space plasmas are taken into account. The detailed interaction of realistic, wave-like cyclic perturbations with the intermediate-shock segments in bow shock flows may lead to unsteady structures composed of (time-dependent) intermediate shocks, rotational discontinuities, and nonlinear wave trains, as in the scenarios proposed by *Markovskii and Skorokhodov* [2000]. The possible relevance of the new bow shock topology with intermediate shocks for space weather phenomena is discussed.

1. Introduction

Many macroscopic phenomena in astrophysical and laboratory plasmas may be described by the equations of magnetohydrodynamics (MHD) [*Landau and Lifshitz*, 1984]. The equations of ideal single-fluid MHD in conservative form are given by

$$\frac{\partial}{\partial t} \begin{bmatrix} \rho \\ \rho \vec{v} \\ \vec{B} \\ e \end{bmatrix} + \nabla \cdot \begin{bmatrix} \rho \vec{v} \\ \rho \vec{v} \vec{v} + I \left(p + \vec{B} \cdot \vec{B} / 2 \right) - \vec{B} \vec{B} \\ \vec{v} \vec{B} - \vec{B} \vec{v} \\ \left(e + p + \vec{B} \cdot \vec{B} / 2 \right) \vec{v} - \left(\vec{v} \cdot \vec{B} \right) \vec{B} \end{bmatrix} = 0. \quad (1)$$

¹Now at Department of Applied Mathematics, University of Colorado at Boulder.

Copyright 2001 by the American Geophysical Union.

Paper number 2000JA000205.
0148-0227/01/2000JA000205\$09.00

These equations have to be supplemented with the divergence-free condition $\nabla \cdot \vec{B} = 0$ as an initial condition. Here ρ and p are the plasma density and pressure, respectively, \vec{v} is the plasma velocity, \vec{B} is the magnetic field, and

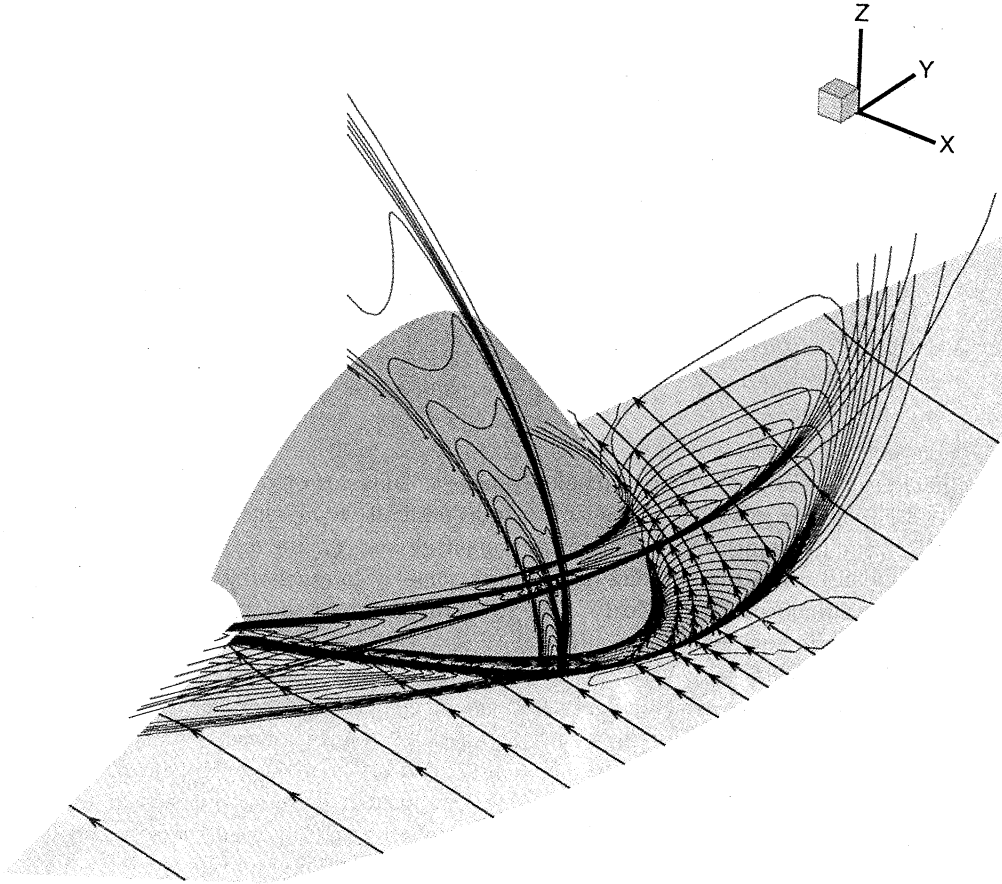


Figure 1. Simulation result of a three-dimensional (3-D) MHD bow shock flow around a perfectly conducting paraboloid surface with strong upstream magnetic field. The flow comes in from the right. Density contours in three planes and magnetic field lines (with arrows) are shown. A complex double-front topology is obtained. The upstream parameters are $\beta = 0.4$, the Mach number $M = v/c = 2.6$ (where c is the sound speed), and the angle between the velocity and magnetic field $\theta_{vB} = 15^\circ$. The upstream velocity is parallel to the x axis, which is the symmetry axis of the paraboloid, and the magnetic field is parallel to the xy plane, which is a plane of symmetry.

$$e = \frac{p}{\gamma - 1} + \rho \frac{\vec{v} \cdot \vec{v}}{2} + \frac{\vec{B} \cdot \vec{B}}{2} \quad (2)$$

is the total energy density of the plasma. I is the unity matrix. The magnetic permeability $\mu = 1$ in our units. We take $\gamma = 5/3$ for the adiabatic index. These equations describe the conservation of mass, momentum, magnetic field, and energy, respectively.

MHD allows for three different anisotropic wave modes: the fast, the Alfvén, and the slow wave, with phase speeds in arbitrary direction x denoted by c_{fx} , c_{Ax} , and c_{sx} , respectively. Corresponding to the three types of waves, the nonlinear MHD equations allow for three different types of shocks, namely the fast, intermediate, and slow shocks.

Important examples of shock phenomena in solar and space plasmas are the bow shocks induced by obstacles in fast plasma streams. Space physics bow shock flows have been studied extensively by observations and numerical simulations, and a rich literature exists on the

Earth's bow shock and magnetosheath induced by the solar wind [Walters, 1964; Spreiter *et al.*, 1966; Song *et al.*, 1990; Phan *et al.*, 1994; Cairns and Lyon, 1996; Yan and Lee, 1996; De Sterck and Poedts, 1999b, 2000; De Sterck, 1999], and on the leading shocks induced by fast solar coronal mass ejections (CMEs) [Sheeley *et al.*, 1985; Steinolfson and Hundhausen, 1990; De Sterck and Poedts, 1999c; De Sterck, 1999].

Recent simulations of stationary three-dimensional (3-D) bow shock flows around perfectly conducting rigid obstacles in MHD plasmas with small dissipation [De Sterck and Poedts, 1999b, 1999c, 2000; De Sterck, 1999] have shown that a new complex double-front bow shock topology (Figure 1) arises when the flow upstream from the obstacle satisfies the following conditions of strong magnetic field B :

$$B^2 > \gamma p \quad \rho v_x^2 > B^2 > \rho v_x^2 \frac{\gamma - 1}{\gamma(1 - \beta) + 1}, \quad (3)$$

where v_x is the velocity along the upstream magnetic field, and $\beta = 2p/B^2$ is the plasma β . We call a state

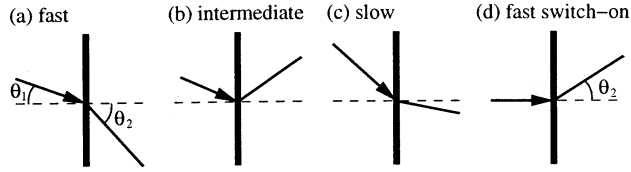


Figure 2. (a–d) MHD shock types. The magnetic field (arrowed) is refracted at the shock (thick). The shock normal is dashed. Region 1 is upstream, and region 2 is downstream.

satisfying these conditions “magnetically dominated”, as opposed to “pressure-dominated.”

For the case of the terrestrial bow shock, for example, statistical study of solar wind parameters at 1 astronomical unit (AU) [De Sterck, 1999; De Keyser *et al.*, 2001] has revealed that condition (3), for which can be expected that space physics bow shocks assume the new double-shock structure, is satisfied overall $\sim 5\%$ of the time, during periods of time that last up to several hours, and more often so around solar maximum. The perfectly conducting rigid paraboloid of Figure 1 can be thought of as crudely modeling the magnetopause in the context of the terrestrial bow shock flow [De Sterck and Poedts, 1999b].

It has been shown that in this new shock topology, particular segments of the shock fronts are of the intermediate MHD shock type [De Sterck and Poedts, 2000; De Sterck, 1999]. Intermediate shocks are known to be completely unstable in ideal MHD [Landau and Lifshitz, 1984] and to be stable in MHD with small dissipation only when perturbations are small enough, in a specific sense, to be explained below in section 2 [Wu, 1988, 1991; Freistuehler, 1991, 1998; Myong and Roe, 1997]. This calls for an investigation of the large-scale stability of the new bow shock topology with intermediate shocks against perturbations, which is done in the present paper.

The paper is organized as follows. Section 2 describes the different types of MHD shocks and their stability properties. Section 3 briefly explains the topology of the magnetically dominated double-front bow shock flow of Figure 1. Section 4 describes two numerical experiments in which an initial stationary magnetically dominated bow shock flow around a conducting paraboloid is perturbed in order to investigate its large-scale stability. Section 5 discusses the results and presents our conclusions.

2. MHD Shocks and Shock Stability

There are three types of MHD shocks (Figure 2), connecting plasma states which are traditionally labeled from 1 to 4, with state 1 superfast ($v_n > c_{fn}$ in the shock frame, where n is the direction of the shock normal), state 2 subfast but super-Alfvénic, state 3 sub-Alfvénic but superslow, and state 4 subslow. The 1–2

fast shock connects a superfast state of type 1 with a state of type 2 and refracts the magnetic field away from the shock normal. The 3–4 slow shock refracts the field toward the normal. A limiting case of the fast shock is the switch-on shock, for which the upstream magnetic field is parallel to the shock normal, while the magnetic field makes a nonzero angle with the shock normal in the downstream state. Intermediate shocks (1–3, 1–4, 2–3, and 2–4) bring a super-Alfvénic upstream plasma to a sub-Alfvénic downstream state, while the magnetic field is flipped over the shock normal: the tangential component of the magnetic field changes sign. All MHD shocks have the property of coplanarity, which means that the downstream magnetic field lies in the plane defined by the upstream magnetic field and the shock normal.

While fast and slow MHD shocks are known to occur in plasma flows, it has been believed for a long time that intermediate MHD shocks are unphysical [Landau and Lifshitz, 1984]. This belief still lingers on, and in most present-day textbooks on space physics and MHD, intermediate shocks are simply left out of the picture when shocks are discussed [e.g., Kivelson and Russell, 1995; Gombosi, 1998]. In the dissipationless, or ideal, MHD system, intermediate shocks are indeed unstable as they disintegrate instantaneously and split up into fast and slow shocks upon arbitrary small perturbation of the magnetic field component out of the plane of coplanarity (by Alfvén waves) [Landau and Lifshitz, 1984; Wu, 1988] (Figure 3). However, recently, it has been shown that intermediate shocks can be stable when dissipation is taken into account [Wu, 1988, 1991; Freistuehler, 1991, 1998; Myong and Roe, 1997]. The precise influence of dissipation mechanisms and magnitudes on the stability of intermediate MHD shocks is complicated, and the analysis remains incomplete. Nevertheless, the following general statements can be made. Intermediate shocks are stable in the dissipative MHD system for wide ranges of the dissipative coefficients [Wu, 1988, 1991; Freistuehler, 1991, 1998; Myong and Roe, 1997]. They can be destabilized by localized Alfvénic perturbations (Figure 3), but only when the total amplitude $I_z = \int B_z dn$ of the noncoplanar

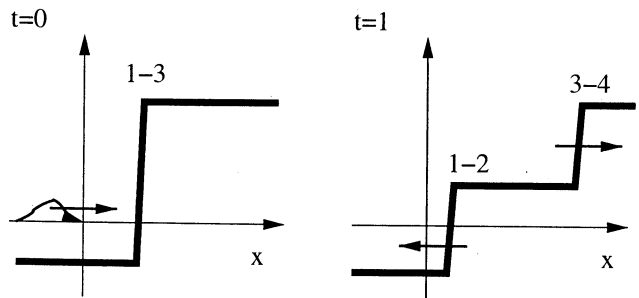


Figure 3. Schematic representation of a 1–3 intermediate shock splitting up into a 1–2 fast shock and a 3–4 slow shock when perturbed by an Alfvén wave.

magnetic field perturbation component B_z , integrated over the perturbation in the direction n normal to the shock, is larger than a critical value [Wu, 1988; Liu, 1991]. This critical value depends on the left and the right states and on the magnitudes of the dissipation coefficients, and it vanishes with vanishing dissipation [Freistuehler, 1998]. The stability issues involving intermediate shocks are due to mathematical properties peculiar to MHD, namely nonstrict hyperbolicity [Wu, 1991; Freistuehler, 1998], nonconvexity [Wu, 1991; Myong and Roe, 1997; De Sterck et al., 1999], and rotational invariance [Freistuehler, 1998; Markovskii, 1999].

The fact that intermediate shocks may be unstable against Alfvén waves, while fast and slow shocks are stable, can intuitively be understood as follows [Liu, 1991; Wu, 1991]. Consider a stationary shock with the upstream state on the left and with n denoting the direction normal to the shock. In the following we discuss the interaction of the shock with a one-dimensional (1-D) wave perturbation that is traveling in the direction of the shock normal n , and thus without variation in the other directions, and that is of localized spatial extent, i.e. a localized wave packet. Consider a fast wave perturbation traveling on the upstream side with speed $v_n - c_{fn}$ and an Alfvénic perturbation traveling with speed $v_n - c_{An}$. The shock is coplanar, and the fast wave perturbation can only carry magnetic field perturbations lying in this plane of coplanarity, while the Alfvén wave carries a perturbation in B_z .

In the case of a 1–2 fast shock a fast upstream wave perturbation with speed $v_n - c_{fn}$ travels toward the shock (rightward) as $v_n > c_{fn}$ upstream (on the left). After interaction with the shock, the fast wave perturbation cannot keep on traveling to the right, as on the downstream side $v_n < c_{fn}$, and the speed is thus negative. Instead, the wave perturbation makes the shock position shift, with the magnitude of the shift proportional to the integrated amplitude of the wave [Liu, 1991]. It is said that the fast wave converges into the fast shock, as $v_n - c_{fn}$ is directed toward the shock on both sides. In contrast, an Alfvénic perturbation traveling with speed $v_n - c_{An}$ approaching the shock from the left is able to continue rightward away from the shock after interaction, as $v_n > c_{An}$ downstream of a 1–2 fast shock. The shock position does thus not need to shift in this case.

For a 1–3 intermediate shock, however, the situation is different. Indeed, as the downstream state is both subfast and sub-Alfvénic, both $v_n - c_{fn}$ and $v_n - c_{An}$ are negative and thus directed toward the shock on the downstream (right) side. The shock is called overcompressive as more than one wave mode converges into the shock. A fast wave perturbation makes the shock position shift again. An Alfvén wave, however, cannot just make the shock shift, because the shock needs to remain coplanar and the Alfvén perturbation is not coplanar. Like the fast wave, the Alfvén wave cannot travel back to the left ($v_n - c_{An} > 0$ upstream), and

neither can it travel to the right ($v_n - c_{An} < 0$ downstream). In ideal MHD the only solution is that upon Alfvénic perturbation the 1–3 intermediate shock splits up into a leftward propagating 1–2 fast shock and a rightward propagating 3–4 slow shock (Figure 3). The B_z perturbation can then propagate between the two shocks. The 1–3 intermediate shock splits up instantaneously upon interaction with even the smallest B_z perturbation. Therefore it is said that it is generically unstable (or “nonevolutionary” [Landau and Lifshitz, 1984]) in ideal MHD.

In dissipative MHD, however, the 1–3 intermediate shock can be conditionally stable. In ideal MHD, shocks are pure discontinuities, but in the dissipative system the shock transition occurs continuously in a thin shock layer. It turns out that the B_z perturbation can be absorbed in the shock layer of the 1–3 intermediate shock as long as $I_z = \int B_z dn$, now integrated over the shock layer, does not exceed a critical value. Hence the solution in the shock layer does not have to be coplanar, whereas for the left and right states it is still required that they are coplanar. For Alfvénic perturbations with supercritical I_z the 1–3 intermediate shock still splits up into a 1–2 fast shock and a 3–4 slow shock (Figure 3), but this happens not instantaneously but after a certain time. It can be concluded that 1–3 intermediate shocks are conditionally stable in dissipative MHD.

In interesting recent work by S.A. Markovskii [Markovskii, 1998a, 1998b, 1999; Markovskii and Skorokhodov, 2000], mainly concerning the interaction of small-amplitude, low-frequency cyclic waves with intermediate shocks, new aspects of the behavior of intermediate shocks have been revealed. Markovskii proposes a mechanism of cyclic oscillatory disintegration of intermediate shocks, which may be time-dependent [Wu and Kennel, 1992a, 1992b], in agreement with the principle of evolutionarity [Markovskii, 1998a, 1998b; Markovskii and Skorokhodov, 2000]. Markovskii’s work is especially relevant for the question of what happens with intermediate shocks when the stability threshold is repeatedly exceeded by perturbations of a cyclic nature [Markovskii and Skorokhodov, 2000]. Such cyclic perturbations are more typical for space plasmas than are single, localized perturbations.

Markovskii [1998a, 1998b, 1999] emphasizes that when the stability threshold is exceeded in a perturbed Riemann problem (a Riemann problem is defined as a problem with an initial condition composed of two constant states separated by a discontinuity), the intermediate shocks in the dissipative system break up, leading to a solution “at large times” which is exactly the same as the solution to the perturbed Riemann problem in a system without dissipation. The threshold for breakup can be exceeded when the integrated amplitude of a localized wave packet perturbation is large enough, as discussed above. For periodic perturbations, for example, sinusoidal waves, of a given amplitude, the threshold will be exceeded (repeatedly, in every single half wave-

length between two points of zero perturbation) when the wavelength is long enough, or equivalently, when the frequency of the wave is low enough. Markovskii focuses much of his analysis on periodic perturbations [Markovskii, 1998b] and says rightfully that for perturbations with low enough frequency the ideal and dissipative systems behave similarly “at large times” for Riemann-like problems.

Markovskii and Skorokhodov [2000] show in 1D simulations that the interaction of small-amplitude low-frequency waves with intermediate shocks can lead to the formation of cyclic unsteady structures composed of (time-dependent) intermediate shocks, rotational discontinuities, and nonlinear wave trains. They emphasize the important point that small-amplitude, almost linear perturbations can result in a strongly nonlinear response due to the repeated accumulation of the perturbation in the shock layer and subsequent nonlinear release when the stability threshold is exceeded. Our simulations do not directly deal with cyclic perturbations, but like in the early 1-D simulations on intermediate-shock stability [Wu, 1987, 1988], we focus for our large-scale 3-D simulations on single, localized perturbations, because those are more simple and easier to analyze and understand. We leave the study of the interaction of bow shocks with cyclic perturbations for future work, but the results obtained by Markovskii and Skorokhodov [2000] will give us guidelines to speculate about what can happen with the intermediate-shock segments in the bow shocks to be described below when they are exposed to cyclic perturbations.

To summarize the discussion on intermediate-shock stability, we can say that fast and slow shocks are stable against Alfvénic perturbations in both dissipative and ideal MHD, because noncoplanar B_z perturbations can be carried away on the downstream side by Alfvén waves, which do not converge into the shocks. Intermediate shocks are unstable in ideal MHD and conditionally stable in dissipative MHD, with instability due to the fact that noncoplanar Alfvén waves converge into intermediate shocks.

The theoretical results on intermediate-shock stability were initially confirmed in 1-D simulations [Wu, 1987, 1988], but 1-D simulations are of limited generality because coplanarity of left and right states has to be imposed explicitly in order to obtain persistent intermediate shocks. The first clear confirmation of the natural occurrence of intermediate shocks in general 3-D MHD flows (where coplanarity is not explicitly imposed) was provided by the simulations of the new complex stationary bow shock topology (Figure 1) [De Sterck and Poedts, 2000; De Sterck, 1999]. However, some concerns regarding the stability and occurrence of intermediate shocks still remain unaddressed. Indeed, it has been argued that intermediate shocks cannot or can only very rarely be observed “at large times” in real plasma flows [Falle and Komissarov, 2001; Myong and Roe, 1997], because initially present intermedi-

ate shocks would disintegrate after short times due to Alfvénic perturbations with supercritical I_z (Figure 3), which are believed to occur in most real plasma flows with small dissipation. Intermediate shocks can certainly not survive for long times in physical situations that can be described by 1-D perturbed Riemann problems. The question whether intermediate shocks can be present “at large times” in more general plasma flows with perturbations is addressed in the present paper. It will turn out that intermediate shocks can be present “at large times”, at least in an intermittent manner, because after having disintegrated, they can be reformed in driven 3-D plasma flows.

3. Stationary 3-D Bow Shock Flows With Intermediate-Shock Segments

In the present section we briefly explain the topology of the magnetically dominated double-front bow shock flow of Figure 1 [De Sterck and Poedts, 2000; De Sterck, 1999]. Figure 4a shows that for a pressure-dominated upstream flow (with a weak upstream magnetic field, for which conditions (3) are not satisfied) the classical single-front bow shock topology (Figure 4c) that is well-known from hydrodynamic bow shocks is obtained. However, Figure 4b shows that for a magnetically dominated flow (with a strong upstream magnetic field, for which conditions (3) are satisfied) the leading bow shock front is followed by a secondary shock front. In this complex topology (Figure 4d), shock fronts AB and DE are 1–2 fast, BD is 1–3 intermediate, and DG is 2–4 intermediate close to point D, evolving into 3–4 slow along the front [De Sterck and Poedts, 1999b; De Sterck, 1999]. The need for this complex topology in the case of magnetically dominated upstream parameters (satisfying conditions (3)) can be explained in terms of the geometrical properties of MHD shocks [De Sterck and Poedts, 2000; De Sterck, 1999; De Sterck et al., 1998; Steinolfson and Hundhausen, 1990]. The intermediate-shock segments arise when a fast switch-on shock occurs at the point B on the leading shock front (Figure 4d) where the upstream magnetic field is perpendicular to the shock front. Conditions (3) are precisely the conditions under which the intrinsically magnetic effect of the switch-on shock can occur [Kennel et al., 1989].

Note that the angle θ_{vB} between the upstream magnetic and velocity fields breaks the symmetry of the flow. In Figure 4b the upstream velocity is oriented slightly upward ($\theta_{vB} = 5^\circ$), leading to an asymmetric flow with the secondary shock on the upward side of the sphere. If the upstream velocity were oriented downward, the secondary shock would be located on the downward side of the sphere. This symmetry breaking does not occur for two-dimensional (2-D) field-aligned flow around a cylinder, for which a symmetrical flow with multiple shock fronts and intermediate-shock seg-

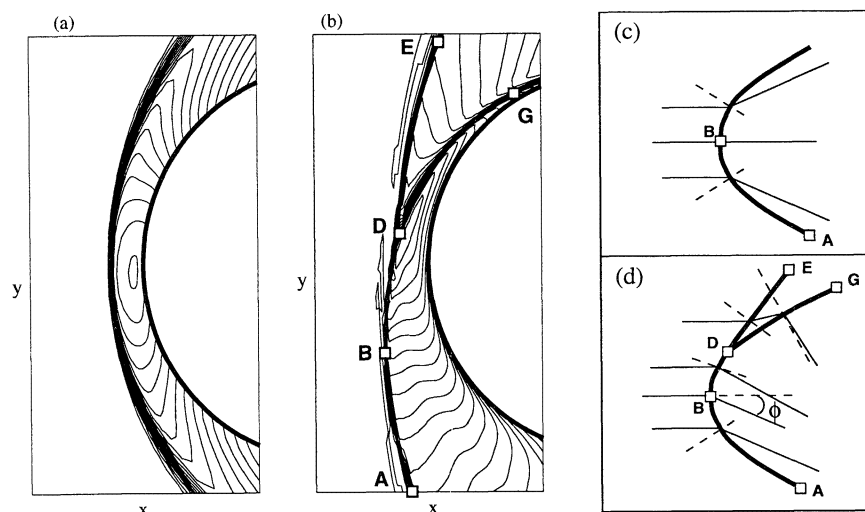


Figure 4. (a–b) Bow shock flows over a sphere (thick solid) and (c–d) the two bow shock topologies in the xy symmetry plane. The flow comes in from the left. Density contours (thin solid) in a plane through the sphere center are shown in Figures 4a and 4b. The incoming magnetic field is aligned with the x axis. Figure 4a shows the pressure-dominated flow ($M_{Ax} = v_x/c_{Ax} = 3.985$, $\beta = 0.4$, $\theta_{vB} = 5^\circ$), and Figure 4b shows the magnetically dominated flow ($M_{Ax} = 1.5$, $\beta = 0.4$, $\theta_{vB} = 3.8^\circ$). In Figures 4c and 4d thick lines are shock fronts, thin lines are magnetic field lines, and shock normals are dashed. Figure 4c shows the pressure-dominated flow topology, and Figure 4d shows the magnetically dominated flow topology.

ments is obtained [De Sterck *et al.*, 1998, 1999; De Sterck and Poedts, 1999a; De Sterck, 1999].

In the simulations the ideal MHD equations are solved using a conservative finite volume shock capturing scheme which is second-order accurate in space and time, employing a slope-limiter approach [De Sterck *et al.*, 2001, 1998; De Sterck, 1999]. The stationary 3-D bow shock flows are obtained starting from a uniform initial condition and by advancing the time-dependent MHD equations until a steady state solution is reached. These steady solutions are then perturbed in the simulations to be described in section 4, by varying the upstream conditions at the boundary in a time-dependent manner.

For reasons of numerical stability, dissipation has to be introduced in shock-capturing numerical schemes. This numerical dissipation vanishes for vanishing grid cell size, but because of limited computer resources, the numerical dissipation is always orders of magnitudes larger than the physical dissipation in space plasmas. Many space plasmas are collisionless, such that the dissipation is provided not by collisions but by electromagnetic effects on kinetic scales [e.g., Burgess, 1995]. In such plasmas the dissipation is often very small, with, for instance, magnetic Reynolds numbers of the order of $10^6 - 10^{12}$. In our numerical simulations the magnetic Reynolds number is of the order of $10^2 - 10^3$. In addition, the numerical dissipation is dependent on the direction in the numerical grid. Within these limitations, numerical dissipation can be interpreted as playing a role analogous to that of a small physical dissipation.

As the stability of intermediate shocks depends on the values of the upstream and downstream state and on the magnitudes of the dissipation coefficients (actually rather on the ratios between the coefficients of the different dissipation mechanisms in a plasma, like viscosity, resistivity, and heat conduction [Freistuehler, 1998]), it would be preferable to perform simulations with explicit discretization of the dissipative terms of the MHD equations. Our results on steady and perturbed bow shock flows are likely to have a general character, however, because qualitatively we obtain the same physical effects using various grid sizes and various numerical schemes, i.e. various effective dissipation and ratios of dissipation coefficients. In anticipation of future simulations with very high resolution and explicit discretization of the dissipative terms, the numerical method employed in this paper is suitable to give a qualitative picture of the general large-scale stability of MHD bow shock flows with intermediate-shock segments, but limited to the parameter regime that can be covered by our numerical schemes using present-day computational resources.

It is conceivable that for realistic levels of dissipation a steady state solution may not exist to the above problem and that a qualitatively different solution may develop, like in the case of the well-known Kelvin-Helmholtz instability that occurs in neutral fluids when the viscosity drops below a critical value. However, we have not found indications for such a bifurcation in our simulations as a function of dissipation. As said above, it is rather the ratios of dissipation coefficients than their absolute values that determine bifurcations in the

stability of intermediate MHD shocks [Freistuehler, 1998] and that could cause a bifurcation in the solution to our bow shock problem. We have to be aware that it remains to be proved that for realistic levels of plasma dissipation the effects that are described in this paper occur.

4. Perturbation of Bow Shock Flows

In the present section we perform two numerical experiments in which we perturb an initial, stationary magnetically dominated bow shock flow around a perfectly conducting, rigid paraboloid with upstream parameters $\rho = 1, p = 0.2, B_x = 1, B_y = 0, B_z = 0, v_x = 1.3 \cos(5^\circ), v_y = 1.3 \sin(5^\circ)$, and $v_z = 0$, or equivalently, $\beta = 0.4, M_{Ax} = 1.295$, and $\theta_{vB} = 5^\circ$. The x axis is an axis of rotational symmetry for the paraboloid. The nose of the paraboloid is located at $(-1, 0, 0)$, and the intersections of the paraboloid with the y axis in the xy plane are located at $(0, -1, 0)$ and $(0, 1, 0)$. When the simulation parameters are scaled back to the physical quantities describing the interaction of a solar wind with speed 450 km s^{-1} with the terrestrial magnetosphere, with the Earth located at $(-0.65, 0, 0)$ such that its distance from the magnetopause along the Sun-Earth line can be taken to be 10 Earth radii R_e and its distance perpendicular to that line can be taken to be $17 R_e$, we find that a unit time interval in our simulations corresponds to a physical time interval of the order of 10 min. The initial flow has the topology of Figure 1. The (total) Alfvén speed $c_A = 1$. The perturbations are chosen large (of the order of the background field) and of sufficiently long duration (several minutes), such that we can be sure that the intermediate shocks become unstable, regardless of the precise values of the dissipation coefficients.

In the first experiment (Figure 5) we perturb the noncoplanar magnetic field component B_z at the inflow boundary with a Gaussian profile in time, centered around $t = 0.5$ and with half-width 0.2 ($B_z = \exp\{-(t - 0.5)/0.2\}^2$). During the initial evolution (from $t = 0.5$ to $t = 1$) the topology changes substantially as the secondary shock front DG disappears. The intermediate-shock segment BD disappears as well, as the leading shock front seems to be entirely of the fast type (xy magnetic field integral curves are refracted away from the normal) between approximately $t = 0.7$ and $t = 1.4$. Between $t = 0.8$ and $t = 1.0$ there are traces of a second discontinuity following the leading shock front, which may indicate that the 1–3 intermediate shock BD has split up into two shocks as in Figure 3. This should be investigated further in simulations on finer grids. Obviously, limitations in computing resources do not allow us to use in the present 3-D simulations the fine resolution that was employed to study the details of intermediate-shock breakup in 1-D simulations [Wu, 1988, 1991; Markovskii and Skorokhodov, 2000]. Also, detailed identification of shock types in

such high-resolution simulations of the perturbed flow would be difficult, compared to the case of the steady flow. In the steady flow the shock types in the xy symmetry plane can be determined easily from the breaking of the magnetic field lines (which lie in the symmetry plane) or from velocity and wave speed profiles along cuts in the xy plane normal to the shock fronts. In the perturbed flow, however, the xy plane is not a plane of symmetry anymore, such that magnetic field lines and directions normal to the shock fronts are not confined to the xy plane but lie in 3-D space, and together with the fact that the shocks are moving and velocities have to be determined relative to this shock motion, this means that detailed identification of shock types would be difficult in such high-resolution simulations. When the perturbation has passed, the 1–3 and 2–4 intermediate-shock segments BD and DG are dynamically reformed starting from $t = 1.4$, and at $t = 11$ the initial steady state topology is recovered.

In these simulations, perfectly conducting rigid wall boundary conditions are imposed on the paraboloid surface (see Figure 1). In this way, the paraboloid acts as an obstacle which makes the bow shock form in the superfast incoming flow. The obstacle forms the bow shock by deflecting the incoming flow. This implies, on the scale of small-amplitude waves, that those waves are reflected from this rigid boundary. The simulation domain boundaries on the sides of the paraboloid are free outflow boundaries, at which the flow quantities are extrapolated such that wave perturbations are not reflected.

In Figure 6 the temporal evolution of the B_z component of the magnetic field is shown along a cut $y = 0$ (see Figure 5) in a grid plane slightly above the xy plane, which is a symmetry plane in the steady initial bow shock flow. The B_z perturbation is imposed at the left roughly from $t = 0$ to $t = 1$ and propagates into the bow shock solution. At $t = 0.4$ a large B_z peak seems to accumulate in the shock layer. Afterward the profile exhibits a lot of variation brought about by the 3-D reaction of the paraboloid obstacle against the perturbation. When the perturbation has long passed, the B_z profile settles back to the initial condition, corresponding to the double-shock bow shock topology with the intermediate-shock segments.

The disintegration of the initial shock and the waves resulting in Figure 6 may be interpreted to correspond qualitatively to the wave structures that are seen in 1-D simulations of the breakup of an intermediate shock perturbed by a localized perturbation as in the works of Wu [1987, 1988] and Markovskii and Skorokhodov [2000]. However, because of the much lower resolution in our 3-D simulation, it is hard to make detailed comparisons. The interaction problem is also more complicated in our simulation because the waves propagate in 3-D space and because the paraboloid surface acts as a wave reflector. Precisely due to the presence of the paraboloid, the bow shock with the interme-

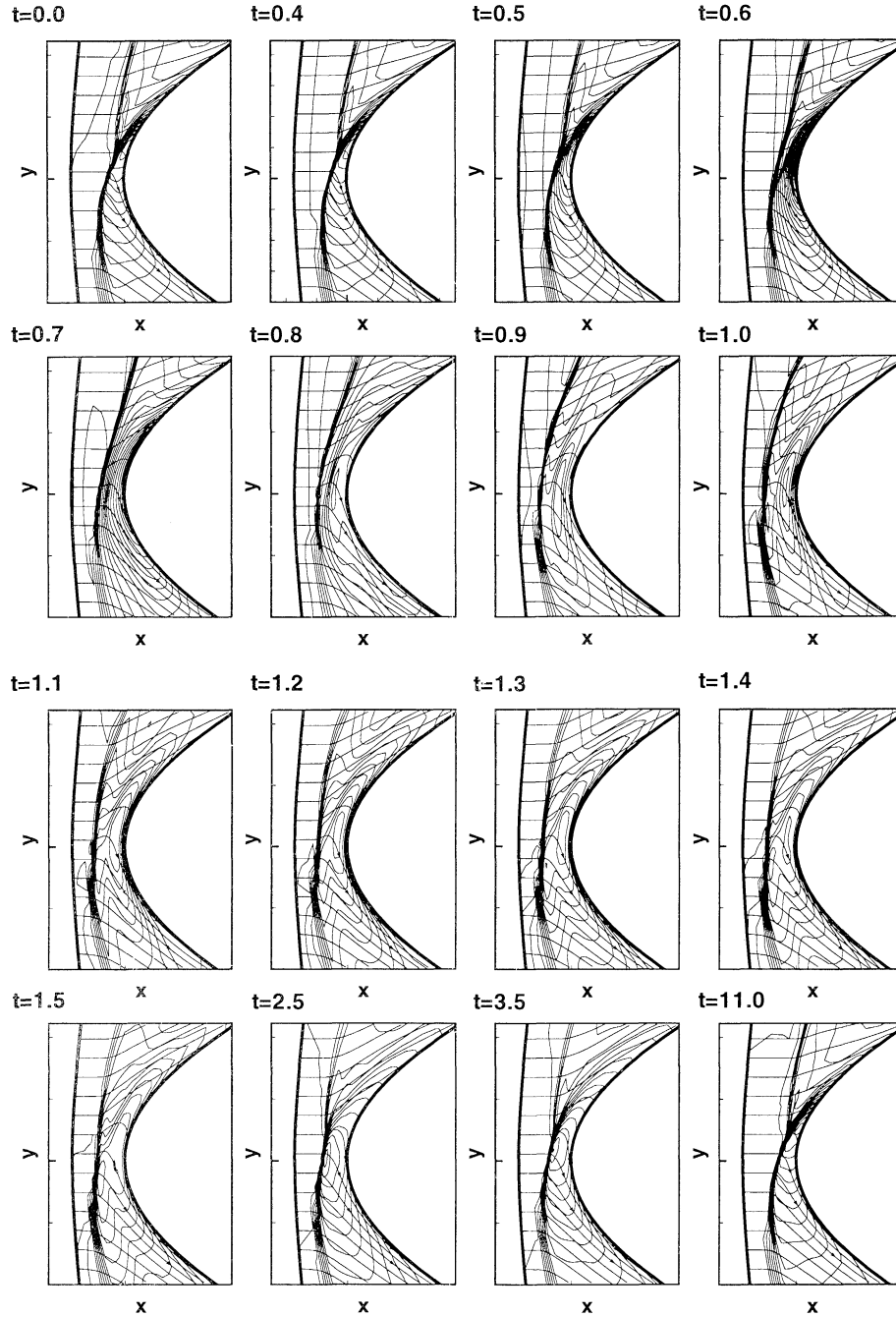


Figure 5. Experiment 1: temporal evolution of the bow shock flow in the xy symmetry plane, during and after perturbation of B_z with a Gaussian profile, centered around $t = 0.5$ and with half-width 0.2. Density contours and integral curves of the magnetic field in the xy plane are shown. Coordinate x ranges from -1.5 to -0.3, and coordinate y ranges from -0.8 to 0.9 ($40 \times 60 \times 60$ grid).

diat segments is reformed after the perturbation has passed, and this makes the final state of our simulation very different from what is obtained in earlier 1-D perturbed Riemann problem simulations [Wu, 1987, 1988; Markovskii and Skorokhodov, 2000].

In our simulations intermediate shocks are reformed exactly as in the initial condition, whereas in 1-D simulations the initial intermediate shocks are not reformed.

In some 1-D cases (e.g., 2–3 shocks) the initial intermediate shock may decay into a time-dependent intermediate shock that evolves toward a rotational discontinuity [Wu and Kennel, 1992a, 1992b; Markovskii and Skorokhodov, 2000]. However, this final rotational discontinuity is not the same as the initial, not time-dependent intermediate shock. For cyclic perturbations, oscillatory disintegration of time-dependent inter-

mediate shocks can be obtained in a 1-D setting, during which the time-dependent intermediate shocks repeatedly transform [Markovskii and Skorokhodov, 2000].

In Figure 7 the temporal evolution of the B_z component of the magnetic field is shown along a cut $y = 0$ in a grid plane slightly above the xy plane, which is a symmetry plane in the steady initial bow shock flow. The cut runs through the initial intermediate-shock seg-

ment, seen by the fact that B_y becomes strongly negative downstream of the shock (see the field lines in Figure 5, intermediate shocks flip the magnetic field lines over the shock normal). The B_y component is not perturbed at the boundary. At $t = 0.6$ the downstream B_z has become positive. Together with the information on shock normal and field line orientation in Figure 5, this indicates that the shock at this location has become of

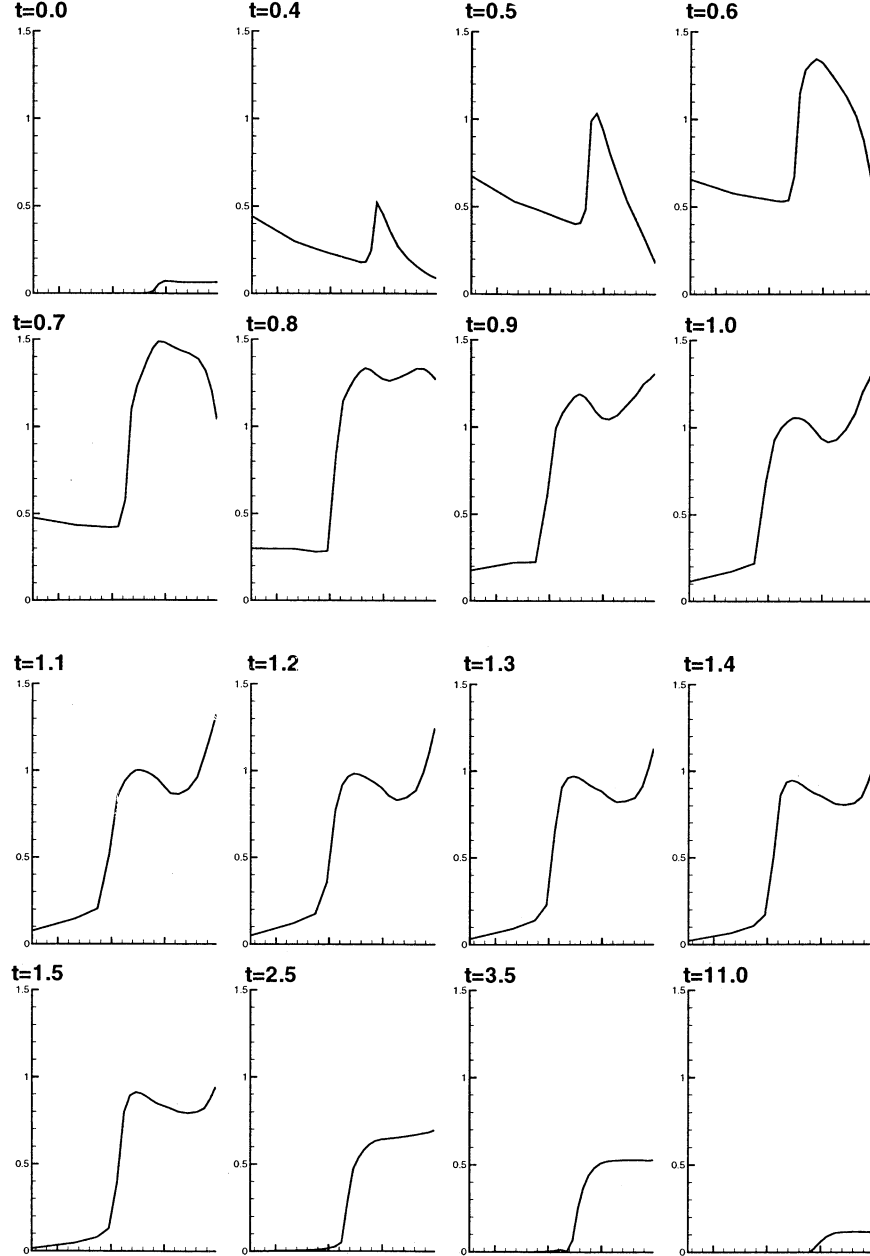


Figure 6. Experiment 1: temporal evolution of the B_z component of the magnetic field along a cut $y = 0$ in a grid plane slightly above the xy plane, which is a symmetry plane in the steady initial bow shock flow. The B_z perturbation is imposed at the left from $t = 0$ to $t = 1$ and propagates into the bow shock solution. At $t = 0.4$ a large B_z peak seems to accumulate in the shock layer. Afterward the profile exhibits a lot of variation brought about by the 3-D reaction of the paraboloid obstacle against the perturbation. When the perturbation has long passed, the B_z profile settles back to the initial condition, corresponding to the double-shock bow shock topology with the intermediate-shock segments.

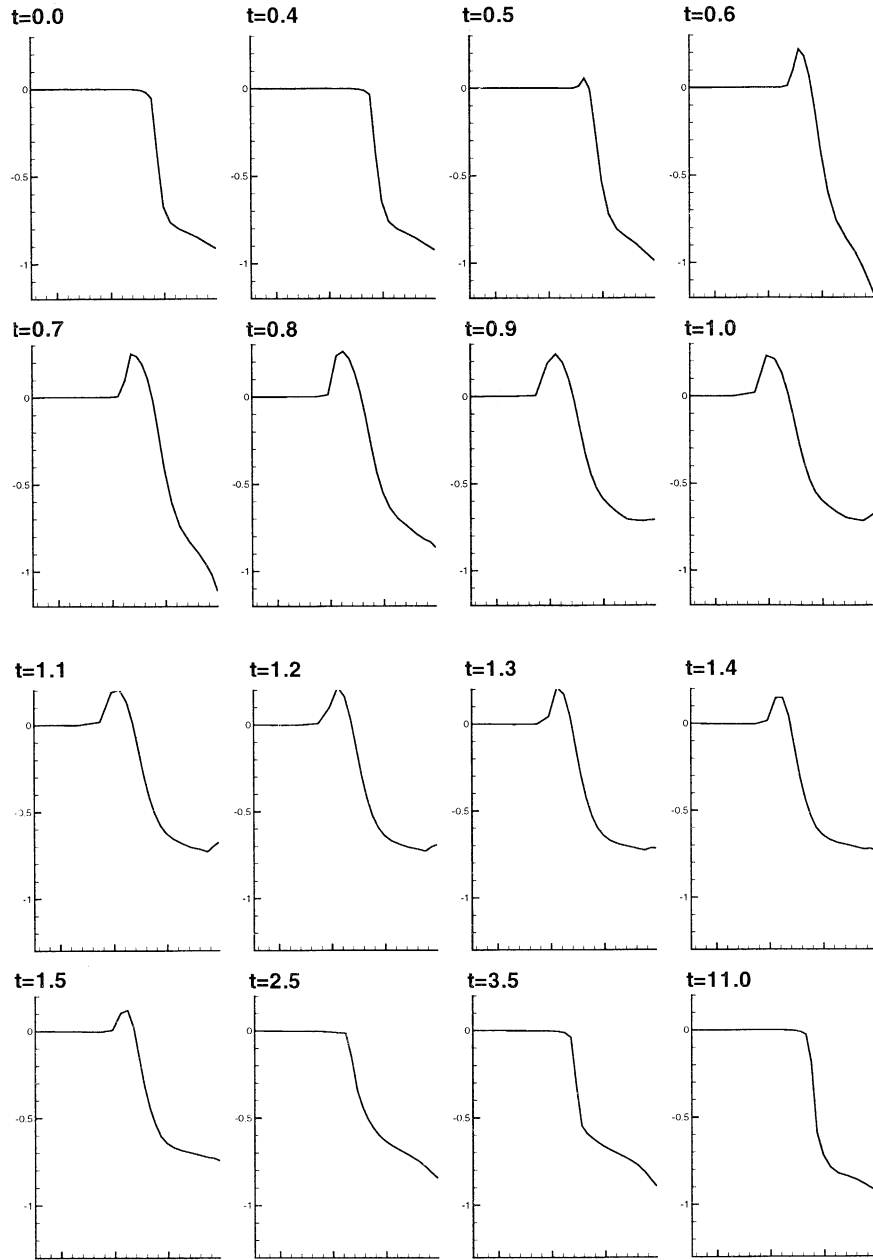


Figure 7. Experiment 1: temporal evolution of the B_y component of the magnetic field along a cut $y = 0$ in a grid plane slightly above the xy plane, which is a symmetry plane in the steady initial bow shock flow. The cut runs through the initial intermediate-shock segment, seen by the fact that B_y becomes strongly negative downstream of the shock (see the field lines in Figure 5; intermediate shocks flip the magnetic field lines over the shock normal). The B_y component is not perturbed at the boundary. At $t = 0.6$ the downstream B_z has become positive. Together with the information on shock normal and field line orientation in Figure 5, this clearly indicates that the shock at this location has become of the fast type (fast shocks refract the magnetic field away from the shock normal): The initial leading intermediate shock has disintegrated, and a fast shock has taken its place. The leading shock remains of the fast type until approximately $t = 2$, after which the perturbation has passed. The intermediate shock is reformed consecutively, as can be seen from the downstream B_z turning negative again from $t = 2.5$ on.

the fast type (fast shocks refract the magnetic field away from the shock normal): The initial leading intermediate shock has disintegrated and a fast shock has taken its place. The leading shock remains of the fast type until approximately $t = 2$, after which the perturbation has passed. The intermediate shock is reformed consec-

utively, as can be seen from the downstream B_z turning negative again from $t = 2.5$ on. For the terrestrial case, along the cut $y = 0$, intermediate shocks thus start to be formed again ~ 10 – 20 min after the perturbation has passed. For the same geometrical reasons as those for which intermediate shocks are formed in the flow of

Figure 1, it is well conceivable that intermediate shocks have been forming at other locations on the bow shock from the very onset of the perturbation on. Indeed, intermediate shocks form near so-called perpendicular points where the upstream magnetic field is perpendicular to the shock front, because they are topologically unavoidable there [De Sterck and Poedts, 2000]. Intermediate shocks are thus likely to have been disintegrating and reforming on various segments of the bow shock during the whole perturbation.

In the second experiment (Figs. 8 and 9) the inflow magnetic field is not directly perturbed, but the large-scale flow is perturbed by gradually rotating the inflow velocity field from the xy plane to the xz plane between $t = 0$ and $t = 1$. From $t = 1$ on the inflow is kept at its new stationary value, which is different from the initial inflow at $t = 0$. In this experiment the final uniform steady inflow state is thus different from the initial inflow state, which is not the case in the first experiment.

In the initial stationary state ($t = 0$) the xy plane exhibits the topology of Figure 4d, while the leading shock front is mainly 1–2 fast in the xz plane, except for the central 1–3 intermediate segment close to the $z = 0$ plane. During the evolution the topology changes sub-

stantially in both the xy and the xz planes, with leading segments of intermediate type changing to fast type but also conversely new intermediate-shock segments being formed dynamically. In the end a new stationary flow is obtained ($t = 11$) with the same topology with intermediate shocks as the original steady flow (Figure 1) but rotated over 90° around the x axis, consistent with the fact that the inflow state has been rotated over that angle too.

This experiment clearly shows that when intermediate-shock segments disappear at certain locations owing to time-dependent changes in the upstream conditions, they are automatically and unavoidably reformed at different locations, owing to the nature of the 3-D flow around the obstacle. Indeed, the geometrical considerations that explain why the topology of Figure 4d arises when the upstream flow is magnetically dominated, imply that as long as the upstream flow is magnetically dominated, the topology of Figure 4d with intermediate shocks will arise near the point B, where the upstream magnetic field is perpendicular to the leading shock front [De Sterck and Poedts, 2000; De Sterck, 1999]. This argument assumes that the intermediate shocks have enough time to form, and in physical plasmas with realistic perturbations it may well be that the intermediate shocks can only exist intermittently.

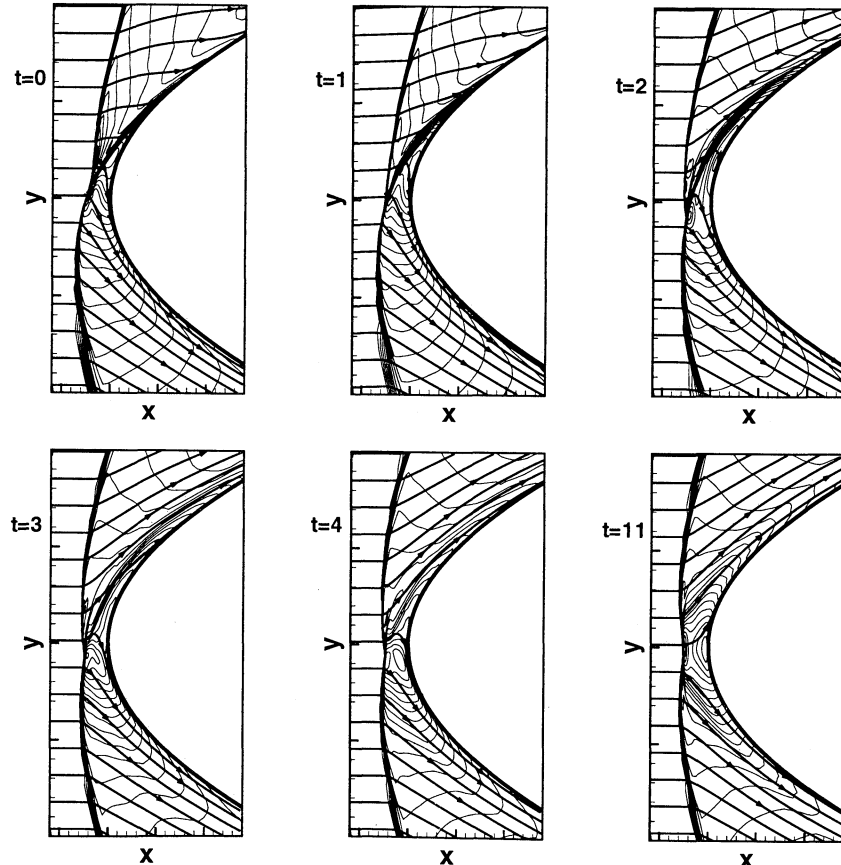


Figure 8. Experiment 2: temporal evolution of the bow shock flow in the xy plane during and after rotation of the inflow velocity field from the xy plane to the xz plane between $t = 0$ and $t = 1$. Density contours and integral curves of the magnetic field are shown. Coordinate x ranges from -1.3 to -0.3, and coordinate y ranges from -1 to 1 ($40 \times 60 \times 60$ grid).

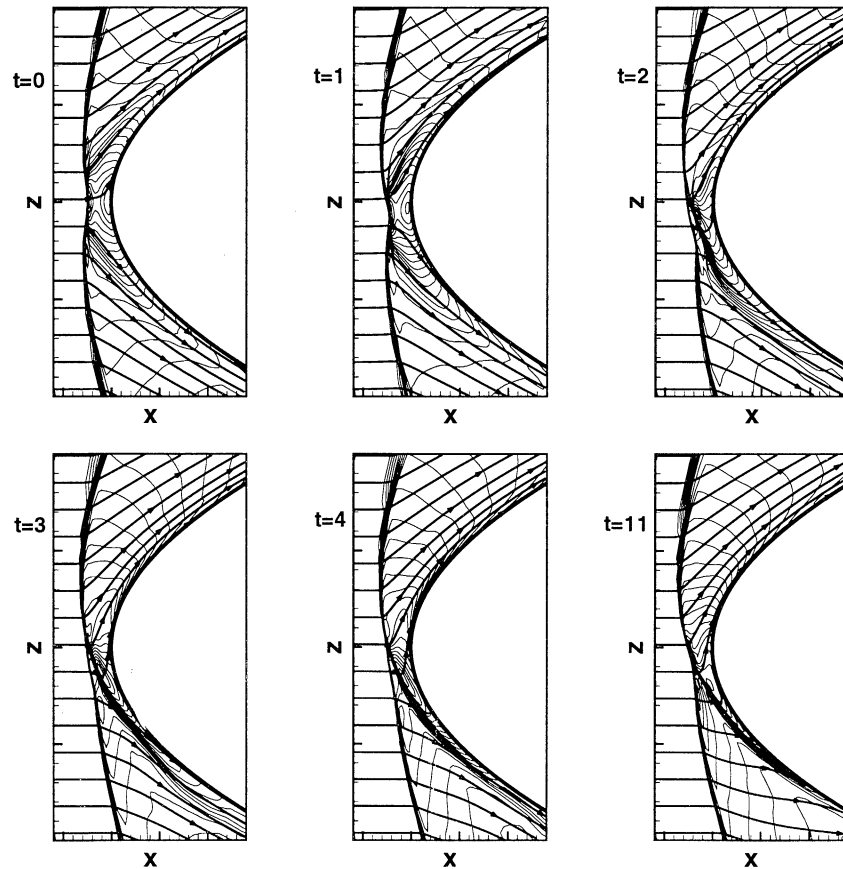


Figure 9. Experiment 2: temporal evolution of the bow shock flow in the xz plane during and after rotation of the inflow velocity field from the xy plane to the xz plane between $t = 0$ and $t = 1$. Density contours and integral curves of the magnetic field are shown. Coordinate x ranges from -1.3 to -0.3, and coordinate z ranges from -1 to 1 ($40 \times 60 \times 60$ grid).

5. Discussion and Conclusion

We have shown that localized perturbations may cause the disintegration of the intermediate shocks in the new magnetically dominated bow shock topology but that the intermediate shocks are dynamically reformed in the driven bow shock flow such that the new topology is regained when perturbations have passed. More generally, we have shown that intermediate shocks can be present “at large times” in plasma flows. It is true that initially present intermediate shocks may disintegrate after short times, owing to Alfvénic perturbations with supercritical I_z , but in 3-D driven flows intermediate-shock segments may be reformed such that they may be present “at large times” as well, at least intermittently.

Qualitatively, we can say that in the context of a given physical plasma with small dissipation the distribution of perturbation amplitudes and frequencies, as related to the critical I_z values and the time of intermediate-shock formation, will ultimately determine if intermediate shocks can occur for long enough times to be observed.

It is a complicated task to quantify such requirements, for example, for the Earth’s magnetosphere

plasma. From our simulation results we can estimate that it would take ~ 30 min for the secondary shock to form in the magnetosheath (Figure 5). Statistical study of solar wind parameters at 1 astronomical unit (AU) [De Sterck, 1999; De Keyser *et al.*, 2001] has revealed that condition (3), for which it can be expected that space physics bow shocks assume the new double-shock structure with intermediate-shock segments, is satisfied overall $\sim 5\%$ of the time, during periods of time that last up to several hours and more often so around solar maximum. Periods of magnetically dominated solar wind thus last long enough for the secondary-shock structure to develop, but during such a period the solar wind is generally quite unsteady such that the secondary shock would not be steady either. It is, for instance, well known that large-amplitude Alfvén waves are generally present in the solar wind [e.g., Hada 1993]. The intermediate shocks can thus be expected to be formed and to disintegrate in an intermittent manner. For the magnetosheath this would mean that the secondary intermediate shock with its associated large density jump (of magnitude up to a factor 2 [see De Sterck and Poedts, 1999b; De Sterck, 1999]) and with its associated strong fieldline and flow deflection, could be ex-

pected to roam the magnetosheath on the quasi-parallel side.

The detailed interaction of realistic, wave-like cyclic perturbations with the intermediate-shock segments in bow shock flows may well lead to unsteady structures composed of (time-dependent) intermediate shocks, rotational discontinuities, and nonlinear wave trains, as in the scenarios proposed by *Markovskii and Skorokhodov* [2000]. It would be very interesting to investigate the reaction of the bow shock flow with intermediate-shock segments to cyclic perturbations as in the work of *Markovskii and Skorokhodov* [2000] in very high resolution simulations, but this is beyond the scope of the present paper.

Markovskii and Skorokhodov [2000] investigate the question of whether intermediate shocks in a 1-D setting, after they have disintegrated under the action of a perturbation, may be reformed and may then disintegrate and reform again repeatedly. In our present simulations, intermediate shocks are indeed reformed after having disintegrated. However, our simulation is 3-D, whereas their work is situated in 1-D space. Our perturbation is localized, but their perturbation is cyclic. These constitute important differences. Indeed, in our simulation the intermediate shocks are reformed, owing to the presence of the 3-D obstacle in the flow and owing to the geometrical properties of MHD shocks in the magnetically dominated regime. In our simulations the reformation of the intermediate shocks thus seems not to be related to their inherent stability properties, whereas inherent instability seems to be the reason for the oscillatory disintegration proposed by *Markovskii* [1998a, 1998b] and *Markovskii and Skorokhodov* [2000].

In the case of space physics plasmas, kinetic effects and the collisionless nature of the plasma complicate the stability of shocks [*Lee et al.*, 1989; *Wu and Hada*, 1991; *Markovskii*, 1999; *Kivelson et al.*, 1991]. It thus remains to be confirmed if intermediate-shock segments would be formed when kinetic effects and realistic dissipation in real space plasmas are taken into account. There is evidence from observations, simulations, and theoretical analysis that intermediate shocks may form in collisionless plasmas [*Kivelson et al.*, 1991; *Wu and Hada*, 1991; *Markovskii*, 1999]. Results on intermediate-shock stability from kinetic simulations do not fully agree with resistive MHD simulations [*Lee et al.*, 1989], but it is unclear how much kinetic effects would change the effects described in this paper. This remains an important topic for future research.

The ultimate test for the applicability of our predictive theoretical results is confrontation with observations. New satellites (Cluster II and Stereo) may provide observations of the new bow shock topology with a secondary shock and with intermediate-shock segments, in the Earth's bow shock flow or in shocks induced by fast CMEs in the solar corona.

It can be speculated as follows that the phenomena described in the present paper may be relevant for

space weather. The MHD solutions were obtained in the idealized setting of flow around a rigid conducting paraboloid surface. It would be interesting to see how the secondary-shock structure influences the inner magnetosphere and the ionosphere in Geospace Global Circulation Model simulations [e.g., *Raeder et al.*, 1998]. When the secondary shock is present, the magnetic field topology in the magnetosheath is changed substantially, which may be important for magnetic reconnection processes at the magnetopause and for storm and substorm mechanisms.

It is generally believed that geoeffective magnetic clouds introduce magnetic field with a negative B_z component into the magnetosheath which, upon arrival at the magnetopause, leads to enhanced reconnection with the Earth's positive B_z magnetic field and in this way contributes to the generation of a magnetic storm. It is not well understood how and how fast this negative B_z field reaches the magnetopause. Our simulation results suggest that magnetic clouds during which condition (3) is satisfied (clouds with a strong magnetic field may indeed satisfy this condition; the January 1997 cloud is a good example [*De Sterck and Poedts*, 1999b; *De Sterck*, 1999; *De Keyser et al.*, 2001]) would not simply propagate through the magnetosheath, but could rather cause a temporary global reconfiguration of the magnetosheath flow, involving leading intermediate-shock segments and a secondary shock in the sheath. When such a magnetic cloud arrives at the bow shock and a secondary shock forms, the characteristic time of this global reconfiguration of the magnetosheath may determine when negative B_z reaches the magnetopause and may thus influence the timing of magnetic storm onset. The possible intermittent formation of intermediate-shock segments and the associated nonlinear wave trains [*Markovskii and Skorokhodov*, 2000] may contribute to enhanced wave activity in the magnetosheath during magnetic cloud events for which condition (3) is satisfied.

These scenarios remain speculative for now, but it would certainly be interesting to investigate them more closely in time-dependent numerical simulations in which the magnetopause is modeled more realistically and in which reconnection can be described, and to look for observational signatures that could confirm it. The Cluster II mission may well provide us with detailed observations of the terrestrial bow shock and magnetosheath region which may confirm the existence of intermediate-shock segments in the bow shock and secondary shocks in the magnetosheath for solar wind parameter values in the magnetically dominated regime (condition (3)). While speculating about these possible consequences of our MHD simulation results, however, we have to keep in mind that it remains to be proved that the phenomena described in this paper occur when kinetic effects and realistic dissipation in real space plasmas are taken into account.

Acknowledgments. The simulations presented in this paper were performed by H.D.S. during a research visit at the High Altitude Observatory (NCAR), which is gratefully acknowledged for its hospitality. S.P. is a Research Associate of the Fund for Scientific Research, Flanders, Belgium.

Janet G. Luhmann thanks Johan De Keyser and another referee for their assistance in evaluating this paper.

References

- Burgess, D., Collisionless shocks, in *Introduction to Space Physics*, edited by M. G. Kivelson and C. T. Russell, pp. 129–163, Cambridge Univ. Press, New York, 1995.
- Cairns, I. H., and J. G. Lyon, Magnetic field orientation effects on the standoff distance of Earth's bow shock, *Geophys. Res. Lett.*, **23**, 2883, 1996.
- De Keyser, J., H. De Sterck, M. Roth, and S. Poedts, Magnetically dominated solar wind in the inner heliosphere, *Space Sci. Rev.*, in press, 2001.
- De Sterck, H., Numerical simulation and analysis of magnetically dominated MHD bow shock flows with applications in space physics, Ph.D. thesis, Katholieke Univ. Leuven, Belgium, 1999.
- De Sterck, H., and S. Poedts, Field-aligned magnetohydrodynamic bow shock flows in the switch-on regime: Parameter study of the flow around a cylinder and results for the axi-symmetrical flow over a sphere, *Astron. Astrophys.*, **343**, 641, 1999a.
- De Sterck, H., and S. Poedts, Stationary slow shocks in the magnetosheath for solar wind conditions with $\beta < 2/\gamma$: Three-dimensional MHD simulations, *J. Geophys. Res.*, **104**, 22,401, 1999b.
- De Sterck, H., and S. Poedts, Complex interacting shock fronts induced by fast CMEs, in *Proceedings of the 9th European Meeting on Solar Physics*, Eur. Space Agency Spec. Publ., ESA-SP-448, 935, 1999c.
- De Sterck, H., and S. Poedts, Intermediate shocks in three-dimensional magnetohydrodynamic bow-shock flows with multiple interacting shock fronts, *Phys. Rev. Lett.*, **84**(24), 5524, 2000.
- De Sterck, H., B. C. Low, and S. Poedts, Complex magnetohydrodynamic bow shock topology in field-aligned low- β flow around a perfectly conducting cylinder, *Phys. Plasmas*, **5**, 4015, 1998.
- De Sterck, H., B. C. Low, and S. Poedts, Characteristic analysis of a complex two-dimensional magnetohydrodynamic bow shock flow with steady compound shocks, *Phys. Plasmas*, **6**, 954, 1999.
- De Sterck, H., A. Csik, D. Vanden Abeele, S. Poedts, and H. Deconinck, Stationary two-dimensional magnetohydrodynamic flows with shocks: Characteristic analysis and grid convergence study, *J. Comput. Phys.*, **166**, 28, 2001.
- Falle, S. A. E. G., and S. S. Komissarov, On the inadmissibility of non-evolutionary shocks, *J. Plasma Phys.*, **65**, 29, 2001.
- Freistuehler, H., Some remarks on the structure of intermediate magnetohydrodynamic shocks, *J. Geophys. Res.*, **96**, 3825, 1991.
- Freistuehler, H., Small amplitude intermediate magnetohydrodynamic shock waves, *Phys. Scr. T*, **74**, 26, 1998.
- Gombosi, T. I., *Physics of the Space Environment, Atmos. and Space Sci. Ser.*, Cambridge Univ. Press, New York, 1998.
- Hada, T., Evolution of large amplitude alfvén waves in the solar wind with beta approximately 1, *Geophys. Res. Lett.*, **20**, 2415, 1993.
- Kennel, C. F., R. D. Blandford, and P. Coppi, MHD intermediate shock discontinuities, 1, Rankine-Hugoniot conditions, *J. Plasma Phys.*, **42**, 299, 1989.
- Kivelson, M. G., and C. T. Russell, *Introduction to Space Physics*, Cambridge Univ. Press, New York, 1995.
- Kivelson, M., et al., Magnetic field studies of the solar wind interaction with Venus from the Galileo flyby, *Science*, **253**, 1518, 1991.
- Landau, L. D., and E. M. Lifshitz, *Electrodynamics of Continuous Media*, Pergamon, Tarrytown, N. Y., 1984.
- Lee, L. C., L. Huang, and J. K. Chao, On the stability of rotational discontinuities and intermediate shocks, *J. Geophys. Res.*, **94**, 8813, 1989.
- Liu, T.-P., On the viscosity criterion for hyperbolic conservation laws, in *Viscous Profiles and Numerical Methods for Shock Waves, SIAM Proc. Ser.*, edited by M. Shearer, pp. 105–114, Soc. for Ind. and Appl. Math., Philadelphia, Pa., 1991.
- Markovskii, S. A., Nonevolutionary discontinuous magnetohydrodynamic flows in a dissipative medium, *Phys. Plasmas*, **5**, 2596, 1998a.
- Markovskii, S. A., Oscillatory disintegration of nonevolutionary magnetohydrodynamic discontinuities, *Sov. Phys. JETP, Engl. Transl.*, **86**, 340, 1998b.
- Markovskii, S. A., Nonevolutionarity of trans-Alfvénic shocks in a magnetized plasma, *J. Geophys. Res.*, **104**, 4427, 1999.
- Markovskii, S. A., and S. L. Skorokhodov, Oscillatory disintegration of a trans-Alfvénic shock: A magnetohydrodynamic simulation, *Phys. Plasmas*, **7**, 158, 2000.
- Myong, R. S., and P. L. Roe, Shock waves and rarefaction waves in magnetohydrodynamics, 1, A model system, *J. Plasma Phys.*, **58**, 485, 1997.
- Phan, T.-D., G. Paschmann, W. Baumjohann, N. Sckopke, and H. Luehr, The magnetosheath region adjacent to the dayside magnetopause: AMPTE/IRM observations, *J. Geophys. Res.*, **99**, 121, 1994.
- Raeder, J., J. Berchem, and M. Ashour-Abdalla, The Geospace Environment Modeling grand challenge: Results from a Global Geospace Circulation Model, *J. Geophys. Res.*, **103**, 14,787, 1998.
- Sheeley, N. R., Jr., R. A. Howard, D. J. Michels, M. J. Koomen, R. Schwenn, K. H. Muehlhaeuser, and H. Rosenbauer, Coronal mass ejections and interplanetary shocks, *J. Geophys. Res.*, **90**, 163, 1985.
- Song, P., C. T. Russell, J. T. Gosling, M. F. Thomsen, and R. C. Elphic, Observations of the density profile in the magnetosheath near the stagnation streamline, *Geophys. Res. Lett.*, **17**, 2035, 1990.
- Spreiter, J. R., A. L. Summers, and A. Y. Alksne, Hydro-magnetic flow around the magnetosphere, *Planet. Space Sci.*, **14**, 223, 1966.
- Steinolfson, R. S., and A. J. Hundhausen, MHD intermediate shocks in coronal mass ejections, *J. Geophys. Res.*, **95**, 6389, 1990.
- Walters, G. K., Effect of oblique interplanetary magnetic field on shape and behavior of the magnetosphere, *J. Geophys. Res.*, **69**, 1769, 1964.
- Wu, C. C., On MHD intermediate shocks, *Geophys. Res. Lett.*, **14**, 668, 1987.
- Wu, C. C., The MHD intermediate shock interaction with an intermediate wave: Are intermediate shocks physical?, *J. Geophys. Res.*, **93**, 987, 1988.
- Wu, C. C., New theory of MHD shock waves, in *Viscous Profiles and Numerical Methods for Shock Waves, SIAM Proc. Ser.*, edited by M. Shearer, pp. 209–236, Soc. for Ind. and Appl. Math., Philadelphia, Pa., 1991.

- Wu, C. C., and T. Hada, Formation of intermediate shocks in both two-fluid and hybrid models, *J. Geophys. Res.*, **96**, 3769, 1991.
- Wu, C. C., and C. F. Kennel, Structural relations for time-dependent intermediate shocks, *Geophys. Res. Lett.*, **19**, 2087, 1992a.
- Wu, C. C., and C. F. Kennel, Structure and evolution of time-dependent intermediate shocks, *Phys. Rev. Lett.*, **68**, 56, 1992b.
- Yan, M., and L. C. Lee, Interaction of interplanetary shocks and rotational discontinuities with the Earth's bow shock, *J. Geophys. Res.*, **101**, 4835, 1996.
-
- H. De Sterck, Department of Applied Mathematics, University of Colorado at Boulder, Campus Box 526, Boulder, Colorado 80309-0526. (desterck@colorado.edu)
- S. Poedts, Centre for Plasma Astrophysics, Katholieke Universiteit Leuven, Celestijnenlaan 200B, 3001 Leuven, Belgium. (stefaan.poedts@wis.kuleuven.ac.be)

(Received June 29, 2000; revised February 16, 2001; accepted March 5, 2001.)